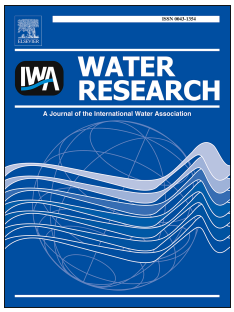

Role of absorber and desorber units and operational conditions for *N*-Nitrosamine formation during amine-based carbon capture

Zimeng Wang, Zhong Zhang, William A. Mitch

PII: S0043-1354(19)31073-5

DOI: https://doi.org/10.1016/j.watres.2019.115299

Reference: WR 115299

To appear in: *Water Research*

Received Date: 9 September 2019

Revised Date: 6 November 2019

Accepted Date: 8 November 2019

Please cite this article as: Wang, Z., Zhang, Z., Mitch, W.A., Role of absorber and desorber units and operational conditions for *N*-Nitrosamine formation during amine-based carbon capture, *Water Research* (2019), doi: https://doi.org/10.1016/j.watres.2019.115299.

Graphical Abstract

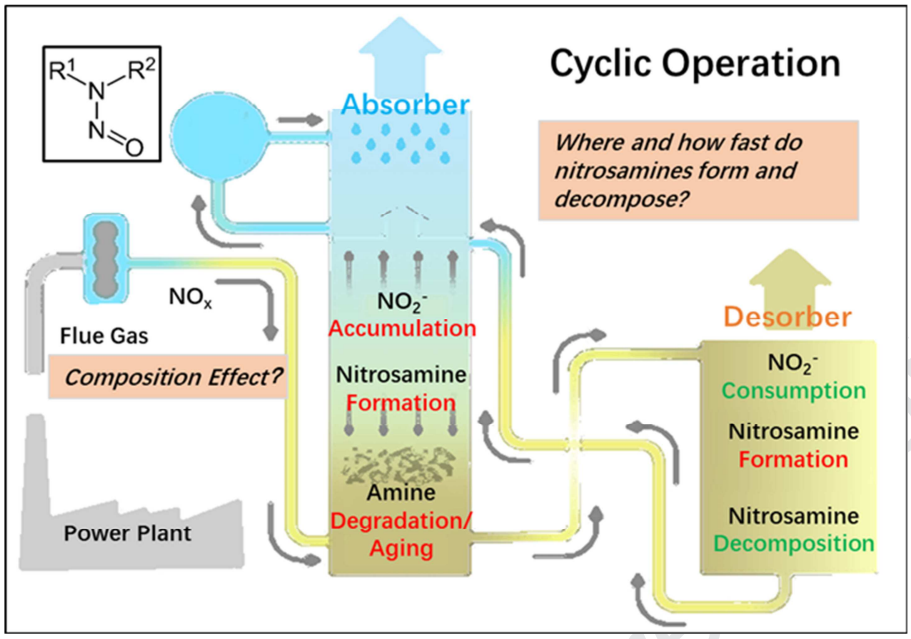

Role of Absorber and Desorber Units and Operational Conditions for *N*-Nitrosamine Formation during Amine-Based Carbon Capture

Zimeng Wang[1,3†], Zhong Zhang[2†] and William A. Mitch[2]*

[1] Department of Environmental Science and Engineering, Fudan University, Shanghai, China

[2] Department of Civil and Environmental Engineering, Stanford University, Stanford, California, United States

[3] Shanghai Institute of Pollution Control and Ecological Security, Shanghai, China.

[†] Those authors contributed equally to this work

*Corresponding author

wamitch@stanford.edu

473 Via Ortega, Stanford, CA 94305

Abstract

The formation of carcinogenic *N*-nitrosamines from reactions between solvent amines and flue gas NO_x is an important concern for the application of amine-based processes to capture CO_2 post-combustion. Using an advanced test rig with interconnected absorber and desorber units, we evaluated the importance for *N*-nitrosamine formation of the desorber relative to the absorber, and any synergism between the two units. Variations in desorber temperature and in flue gas composition indicated that *N*-nitrosamine formation from fresh monoethanolamine (MEA) occurred predominantly in the absorber. *N*-nitrosamine formation was driven by high NO_2 and O_2 flue gas concentrations, although NO also contributed. In contrast, *N*-nitrosamine formation from piperazine (PZ) was driven by reactions with nitrite in the heated desorber, and accelerated concurrent with nitrite accumulation. A complementary experiment simulating aged MEA solvent (high nitrite, 1.5% sarcosine as a proxy of secondary amine degradation products) suggested the desorber becomes an order of magnitude more important than the absorber for *N*-nitrosamine formation. For fresh MEA solvent, increasing the desorber temperature from 110 °C to 130 °C promoted thermal decomposition of *N*-nitrosamines, reducing *N*-nitrosamine accumulation rates two-fold. Compared to the test rig, the prevailing practice of using separate absorber columns and autoclave-like treatments to mimic desorber units predicted the direction,

but underestimated the magnitude of *N*-nitrosamine formation. Because *N*-nitrosamine accumulation rates are the net result of competing formation and thermal decomposition processes, use of continuously cycling test rigs may be necessary to understand the impacts of different operating conditions.

1. Introduction

Efforts to capture and sequester CO_2 emissions have focused on fossil fuel-fired power plants as the largest point sources of CO_2. With decades of full-scale experience from CO_2 capture pre-combustion, amine-based scrubbing processes remain the most mature technology for future post-combustion CO_2 capture applications (Rochelle, 2009; Barzagli et al., 2016). In amine-based processes, flue gases pass through an absorber unit (~45 °C) in which a countercurrent aqueous amine-based solvent (e.g., monoethanolamine (MEA)) reacts with gaseous CO_2 to form a covalent carbamate (for primary and secondary amines; equation 1 for a primary amine) or ionic bicarbonate complex (for tertiary amines and some sterically-hindered amines). The CO_2-rich amine solution then proceeds to a desorber unit, where high temperature (~110-150 °C) reverses the reaction, regenerating lean amine and releasing CO_2 for geological storage. Amine-based capture pilot plants and test facilities have been operated in North America, Europe and Australia (Cousins et al., 2012; Maree et al., 2013; Clark and Herzog, 2014; Idem et al., 2015).

$$2\ RNH_2 + CO_2 \leftrightarrow RNHC(=O)O^- + RNH_3^+ \quad (1)$$

An emerging concern for amine-based post-combustion CO_2 capture is the formation of potentially carcinogenic *N*-nitrosamine byproducts resulting from reactions between flue gas NO_x and the amines (Reynolds et al., 2012; Dutcher et al., 2015; Yu et al., 2017; Chen et al., 2018). *N*-Nitrosamines accumulating in the solvent may contaminate downwind airsheds and water supplies after being stripped from the solvent and/or washwater units into the CO_2 capture process exhaust gas (Dai et al., 2012; Dong et al., 2019; Glover et al., 2019; Zhao et al. 2019). Our previous results using a laboratory-scale absorber unit indicated that N_2O_3 (formed by the reaction of NO with NO_2) is the dominant nitrosating agent within the absorber (equation 2) (Dai and Mitch, 2014). N_2O_3 can either nitrosate amines or hydrolyze to produce nitrite (equation 3). Laboratory-scale experiments using autoclave-like systems to mimic the high temperature, pressure and pH conditions of desorber units (~110-150 °C, 2 bar, pH ~10) have indicated that these conditions can promote nitrosation of amines by nitrite (Goldman et al., 2013; Chandan et al., 2013; Fine et al., 2014), potentially by N_2O_3 formed via the reverse of equation 3, or catalysis by formaldehyde (Keefer and Roller, 1973; Challis and Kyrtopoulos, 1976; Casado et al., 1984; Zhou et al., 2018) carbamates (Sun et al., 2011; Goldman et al., 2013; Fine et al., 2014a) or $O{=}N\text{-}OCO_2^-$ (Yu et al., 2017; Shi et al., 2017). Laboratory-scale absorber column or autoclave-

like systems have demonstrated that *N*-nitrosamine formation follows the order: secondary amines > tertiary amines >> primary amines (Dai and Mitch, 2013). While N_2O_3 can nitrosate all three amine categories, only secondary *N*-nitrosamines are stable (Mirvish, 1975); stable *N*-nitrosamine formation from primary and tertiary amines requires initial formation of secondary amines as byproducts of oxidative degradation (Strazisar et al., 2003; Gouedard et al., 2012). Trace level dissolved Cu can significantly promote *N*-nitrosamine formation from primary amines that are prone to such oxidative degradation (Wang and Mitch, 2015).

$$R_2NH + N_2O_3 \rightarrow R_2N\text{-}N{=}O + H^+ + NO_2^- \quad (2)$$

$$N_2O_3 + H_2O \leftrightarrow 2\ NO_2^- + 2\ H^+ \quad (3)$$

The reliance of previous laboratory-scale research (Dai et al., 2012; Dai and Mitch, 2013; Goldman et al., 2014; Chandan et al., 2013; Fine et al., 2014a; Wang and Mitch, 2015; Voice et al., 2015; Saeed et al., 2018) on separate absorber columns and autoclave-like mimics for desorber units results from the difficulty of constructing flow-through desorber units due to their high temperature and pressure conditions. However, there are several reasons to suspect that the interplay between absorber and desorber units not captured by such laboratory-scale systems may be important. First, it is unclear whether the high temperature and pressure conditions within desorber units promote amine degradation leading to amine-based precursors that are

easier to nitrosate within absorber units. Second, nitrite produced in the absorber column can be consumed in the desorber columns via nitrosation of amines. If this nitrosation results from reactions with N_2O_3 formed via nitrite (the reverse of equation 3), *N*-nitrosamine formation would be expected to be second-order in nitrite (Mirvish, 1975). However, other research has indicated that nitrite-associated *N*-nitrosamine formation can be first-order in nitrite when associated with formaldehyde (Keefer and Roller, 1973), another oxidative degradation product of amines such as MEA (Chi and Rochelle, 2002; Dai et al., 2012; Gouedard et al., 2012; Ge et al., 2014). When laboratory-scale evaluations autoclave samples retrieved after several passes through isolated absorber columns, the nitrite accumulation likely is significantly faster than in pilot-scale facilities encompassing inter-connected absorber-desorber systems, where nitrite is consumed during each pass through the desorber units. If *N*-nitrosamine formation in the desorber is second-order in nitrite, the accumulation of nitrite in laboratory-scale systems would have the effect of overemphasizing the importance of *N*-nitrosamine formation within desorber units relative to that in absorber units. Finally, the high temperature conditions in desorber units may mitigate *N*-nitrosamine accumulation rates in solvents by promoting *N*-nitrosamine decomposition (Voice et al., 2015; Tall and Zeman, 1985; Fine et al., 2014b), an effect not captured in laboratory-scale systems employing only absorber columns.

While pilot-scale systems could fill this gap, there are few of these units and they often are devoted to long-term tests without systematic variation of operational parameters. Several laboratory-scale experimental platforms mimicking absorber-desorber cycling, including the Integrated Solvent Degradation Apparatus (ISDA) and the MiniPlant, have been employed to evaluate net *N*-nitrosopiperazine formation from piperazine (PZ) solvents spiked with nitrite (Voice et al., 2015; Saeed et al., 2018; Ali Mazari et al., 2019). When the desorber mimic within these systems was operated at 120 °C, high to near quantitative yields of *N*-nitrosopiperazine from nitrite reactions were coupled with its first-order decay (half-life ~ 1.5 days). In separate batch reactor studies of *N*-nitrosopiperazine decomposition as a function of temperature, the half-life of *N*-nitrosopiperazine decomposition dropped to ~7 hours at 150 °C (Fine et al., 2014b). However, these experiments did not apply NO_x to an absorber mimic to capture the interplay between these two units. Additional studies (Haugen et al., 2012; Einbu et al., 2013; Vevelstad et al., 2017) used one of the five advanced test rigs designed by SINTEF (Norway) incorporating inter-connected, continuously cycling absorber and desorber columns developed as part of the Amine Technology Qualification Program (TQP Amine) under the CO_2 Capture Mongstad Project (CCM) in Norway (de Koeijer et al., 2011; Hamborg et al., 2014). These studies using 5 M (30% by weight) MEA solvent were performed as a continuous 14-week campaign that was

104 divided into four test conditions: baseline (desorber temperature at 120 °C, 12% O_2 and 5 ppmv
105 NO_x), high O_2 (18%), high desorber temperature (140 °C), and high NO_x (50 ppmv). The overall
106 degradation rate of MEA did not vary significantly throughout the campaign. *N*-Nitroso-(2-
107 hydroxylethyl)glycine constituted ~50% of the total *N*-nitrosamines, with most of the remainder
108 uncharacterized. Increasing the desorber temperature from 120 °C to 140 °C reduced the level of
109 total *N*-nitrosamines by 50%, indicating thermal degradation of *N*-nitrosamines. After 14 weeks
110 of operation, increasing NO_x concentrations did not increase total *N*-nitrosamine concentrations,
111 suggesting that this concentration may reach steady-state over long timescales.

112 The goal of this study was to further evaluate the importance of inter-connected absorber and
113 desorber units for *N*-nitrosamine formation using another one of the five advanced test rigs
114 developed under the CCM program. Our study focused on MEA as the benchmark primary
115 amine solvent in the industry, with limited comparison to piperazine (PZ) as an example
116 secondary amine of interest as a solvent component (Bishnoi and Rochelle, 2000). Rather than
117 varying conditions with one solvent over prolonged periods, we chose to use fresh solvent for
118 each experiment to better control the composition of the solvent and thereby isolate the
119 importance of reaction conditions from complications associated with solvent evolution.
120 However, an experiment was conducted with a synthetic aged MEA solvent consisting of fresh

MEA spiked with nitrite and a model secondary amine to mimic the effects of secondary amines expected to accumulate within MEA over prolonged solvent usage. The first objective was to assess the effect of flue gas conditions on *N*-nitrosamine accumulation rates in fresh MEA solvent, and whether higher temperatures in desorber units could mitigate these *N*-nitrosamine accumulation rates. The second objective was to compare the relative importance of the absorber and desorber units for *N*-nitrosamine formation with fresh MEA and PZ solvents and with a synthetic aged MEA solvent. The third objective was to evaluate the extent to which *N*-nitrosamine formation differed between experiments conducted with conventional laboratory-scale systems (i.e., separate absorber column treatment followed by autoclave-like treatment to mimic desorber column treatment) and treatment conducted within the test rig incorporating continuous treatment by interconnected absorber and desorber columns.

2. Materials and Methods

2.1. Chemicals

Deionized water was used for all the experimental procedures including preparation of solvent solutions, rinsing the test rig, and processing of liquid samples. Solvent solutions included 5 M (30% by weight) MEA (Sigma-Aldrich, ≥ 99%, with ≤ 0.5% water and ≤ 10 mg/kg

Fe), 1 M PZ (Sigma-Aldrich ReagentPlus®, 99% with ≤ 1 % water). While the MEA concentration was relevant to industrial operations (Reynolds et al., 2012; de Koeijer et al., 2011), a lower PZ concentration than that recommended by other authors (Goldman et al., 2013; Nielsen et al., 2013; Cousins et al., 2015) was used due to concerns about the low solubility of PZ at room temperature (Freeman et al., 2010) resulting in clogging of the test rig (Haugen et al., 2012). High purity solvents were used rather than industrial solvents to maximize control over the solvent composition. The technical grade MEA solvents used in industry may contain readily nitrosatable secondary amine impurities, and secondary amines are expected to accumulate as products of oxidative degradation of MEA (Strazisar et al., 2003; Fostas et al., 2011; Gouedard et al., 2012; Vevelstad et al., 2013). An additional experiment employed a synthetic aged MEA solvent consisting of 5 M MEA spiked with 3 mM nitrite and 75 mM sarcosine (Sigma-Aldrich 98%), a model secondary amine. The nitrite concentration approximates the level observed in a previous pilot test involving a MEA solvent (Strazisar et al., 2003). The sarcosine concentration approximates the level of the secondary amine, *N*-(2-hydroxyethyl)glycine, measured as the major secondary amine degradation product to have accumulated in 5 M MEA solvent over 14 weeks of operation in a previous pilot test (Einbu et al., 2013). Praxair 99.9% N_2, CO_2, and O_2,

and NO (2500 ppmv diluted in N_2) and NO_2 (2500 ppmv diluted in N_2), and sodium nitrite (Sigma Aldrich, ACS reagent, >97%) were used as received.

2.2. CO_2 capture test rig

The test rig is a semi-automated unit (1.4 m long × 0.7 m wide × 2 m high) controlled by a computer using a LabView (National Instrument, TX) interface via numerous temperature, pressure, flow and liquid level sensors (photograph shown in Figure S1). The total volume of amine solvent used in a typical experiment was approximately 5 L. Salient features of this complex unit are summarized in Figure 1. Briefly, parts of the rig in contact with gases or liquids are constructed primarily of 316 grade stainless steel with minor use of Teflon and glass. The rig contains absorber and desorber columns (5.1 cm diameter × 1.54 m high) each filled to a depth of 30 cm and each operated in a countercurrent fashion, with amine solvent flowing down and gases flowing up. Identical cushion columns were connected to the absorber and desorber columns by gravity flow. A peristaltic pump recirculates the amine solvent through the absorber unit at 10 L/h via a heated water bath to maintain the solvent at 45 °C. The synthetic flue gas was concocted by mixing N_2, O_2, CO_2, NO_2 and NO using mass flow controllers. Heat tracing and a blower downstream of the gas mixing point pre-heated the fresh and recirculated gases to 45 °C. Another peristaltic pump at the bottom of the absorber column delivered the absorber solvent to

171 the top of the desorber unit at 3.5 L/h. The desorber temperature was controlled by adjusting the
172 duty of an electrical heater at its bottom. The desorber pressure was automatically regulated at
173 2.5 bar by a pressure release valve at the top of the desorber column. Lean solvent was returned
174 to the top of the absorber column by this column pressure. By adjusting the flowrate of the
175 peristaltic pump conveying rich solvent from the absorber to the desorber, together with a valve
176 controlling the flow of lean solvent back to the absorber column, approximately equal volumes
177 of solvent could be maintained in each column. Note that the pressure regulator at the top of the
178 desorber unit prevented the release of most of the CO_2 liberated from the solvent in the desorber.
179 As this CO_2 and the lean solvent flowed back to the absorber unit, it passed through a heat
180 exchanger, where heat was transferred to the rich solvent being pumped from the bottom of the
181 absorber to the top of the desorber unit. The cooling of the lean solvent contributed to the re-
182 absorption of CO_2 into the lean solvent.

183 The overall gas flowrate applied to the absorber column was 3500 L/h, a 260:1 v/v gas-to-
184 liquid ratio approaching those employed in practice (Figure 1). However, only 0.37 L/min (22
185 L/h) of this flow represented fresh flue gas; the remainder was recirculated gas (~159 recycle
186 ratio). The gas recycling was employed to reduce gas consumption during pilot experiments,
187 which would otherwise consume dozens of compressed gas cylinders. The recirculating system

achieved CO_2 loadings relevant to lean and rich MEA and PZ solvents (see below). NO_2 is prone to absorption into the liquid solvents (Fine and Rochelle, 2014) and NO can be oxidized by O_2 to NO_2, particularly on the wetted surfaces within the absorber (Finlayson-Pitts et al., 2003). Therefore, the NO_x composition in the combined fresh influent and recirculated gases contacting the absorber may differ from that in the fresh influent gas. It is challenging to calculate or measure the actual NO and NO_2 concentrations in the absorber and to evaluate their removal during each passage through the absorber. However, we expect significant depletion of NO_2 by absorption into the solvent, while the NO concentration should be less affected, approximating the level applied in the fresh influent gas (Dai et al., 2012), which was also consistent with our results in experiments 1-7 that nitrite accumulation rates were much more sensitive to the input of NO_2 than NO. Regardless, we could safely expect that the NO_x concentrations should be proportional to their dose rates from the stock gas cylinders, so that the variations of the NO and NO_2 dose rates could provide insights into the effects of varying their concentrations. Nonetheless, the experimental plan encompassed high NO_2 concentrations in the fresh influent gas to approximate the NO_2 concentrations expected in the absorber influent if all of the NO_2 were absorbed during each pass through the absorber (see below).

2.3. Test rig operation

The experiments were designed to compare the rates of *N*-nitrosamine accumulation under different flue gas composition and temperature conditions. The experimental duration was selected to be 4 days as it enabled the accumulation of *N*-nitrosamines at measurable concentrations and allowed systematic variation of experimental conditions over reasonable timescales without significant modifications to the solvent composition expected from solvent degradation over prolonged use. Test rig experiments commenced with only N_2 and CO_2 in the flue gas for 12-24 h, during which the temperature, pressure and flowrates were closely monitored to ensure that they approached steady-state. Throughout the experiments, the rich and lean CO_2 loadings stabilized at 0.5 and 0.2 mol CO_2/mol MEA, respectively, and at 0.98 and 0.71 mol CO_2/mol PZ, respectively. The experimental time and monitoring of *N*-nitrosamine and nitrite accumulation commenced upon the addition of O_2, NO and NO_2 to the influent synthetic flue gas. Liquid samples were collected from the rich amine flowing from the absorber and from the lean amine flowing from the desorber (Figure 1); the first 10 mL of each sample was discarded. Evaporation of the liquid over time was compensated by adding freshly prepared amine solvent twice per day, and the total evaporative loss of the solvent volume during a typical 4-day experiment was <15%. In a few experiments, the desorber was initially maintained at the same 45°C temperature as the absorber, but was then heated to 110 °C partway through the

222 experiment; the temperature ramp and stabilization occurred within 30 min. Thorough rinsing
223 and cleaning (at least three times) using deionized water were performed after each experiment.

224 *2.4. Experimental conditions*

225 Table 1 provides the concentrations of constituents tested in the influent flue gases. Some
226 experiments were performed with the desorber temperature at the same 45 °C temperature as the
227 absorber to isolate the extent of *N*-nitrosamine formation attributable to the absorber unit only.
228 Desorber temperatures of 110 °C and 130 °C were evaluated as baseline and high temperature
229 conditions. Although higher temperatures have been considered for some solvents (e.g., 150 °C
230 for PZ) (Fine et al., 2014; Vevelstad et al., 2013, 2014), 130 °C was the upper limit for the test
231 rig, and could only be reached for a limited number of MEA experiments before the seals burst.
232 Experiments were conducted with O_2/CO_2 ratios of 3 (12% O_2 and 4% CO_2), relevant to natural
233 gas, and 0.18 (2.4% O_2 and 13.5% CO_2), relevant to coal combustion (Table S1) (Versteeg et al.,
234 1996).

235 NO_x concentrations varied across two orders of magnitude. While the NO concentration is
236 expected to exceed that of NO_2 in authentic flue gases (Dai et al., 2012), experiments with equal
237 or higher NO_2 concentrations were conducted to indicate the importance of NO_2. Moreover, as
238 mentioned previously, significant absorption of NO_2 into the solvent is expected. Experiments

involving high NO_2 concentrations (e.g., experiments 6, 7, 14 and 15 in Table 1) provide a conservative estimate of the potential importance of NO_2 absorption into the solvent. For example the experiment involving simulated aged MEA solvent applied 320 ppmv NO_2 and 18 ppmv NO (experiments 14 and 15); if all of the NO_2 were absorbed during each pass through the absorber unit, the NO_2 concentration in the combined fresh influent and recirculated gas reaching the absorber would be 2 ppmv. High NO_2 influent gas concentration experiments were limited due to the high cost associated with concentrated NO_2 gas cylinders.

To evaluate the extent to which prolonged autoclaving of absorber samples as a mimic of desorber treatment could predict the *N*-nitrosamine formation occurring in the test rig (where there is continuous cycling between the absorber and desorber units), selected rich amine samples collected from the effluent of the absorber unit were immediately heated to 110 °C in an autoclave for 3 h. After the thermal treatment the sample vials were cooled immediately in a water bath. Total *N*-nitrosamine concentrations were measured before and after the autoclave treatment.

2.5. Analyses

Nitrite was analyzed with the *N*-(1-naphthyl)-ethylenediamine dihydrochloride colorimetric method (Clesceri et al., 1998). CO_2 loadings of solvent amines were measured with

256 a barium titration method (Weiland and Trass, 1969). Because an array of poorly characterized
257 *N*-nitrosamines may form from the degradation products of primary amines (Einbu et al., 2013;
258 Gouedard et al., 2012), a total *N*-nitrosamine (TONO) analysis was used as the primary
259 analytical method (Dai et al., 2012). Briefly, after pretreatment with sulfamic acid to remove
260 nitrite, a sample was injected into a heated reaction chamber containing an acidic tri-iodide
261 solution, which causes cleavage of the N-NO bond in *N*-nitrosamines. The liberated NO is
262 purged from the reaction chamber by N_2 into a chemiluminescence detector (EcoPhysics CLD
263 88sp). The total *N*-nitrosamine concentration is quantified based upon the moles of NO liberated,
264 using *N*-nitrosodimethylamine (NDMA) to develop a standard curve.
265
266 **3. Results and Discussion**
267 *3.1. Baseline conditions*
268 Using fresh 5 M MEA solvent, duplicate experiments were conducted under the baseline
269 conditions reflecting typical influent flue gas relevant to a natural gas-fired power plant with
270 NO_x reduction technologies: absorber column at 45° C, desorber column at 110° C, 18 ppmv NO,
271 2 ppmv NO_2, and a O_2/CO_2 ratio of 3 (experiments 1a and 1b in Table 1). NO_x-free control
272 experiments verified that the rig did not shed any nitrosamines or nitrite, indicating that the

rinsing protocol using DI water between experiments was effective. The accumulation rates of both nitrite and total *N*-nitrosamines were linear over 4 d (Figure 2a). Linear regression yielded nitrite (0.90 and 0.94 μM/h) and total *N*-nitrosamine (0.055 and 0.059 μM/h) formation rates that were highly repeatable between the experimental duplicates (Table 1); the results of additional replicate experiments are provided in the Supporting Information (Table S2). There was no significant difference between the nitrite and total *N*-nitrosamine concentrations (Figure 2a) measured in the lean solvent (sample port A in Figure 1) or the rich solvent (sample port B). This similarity is reasonable because the time to complete a cycle through the absorber and desorber treatment units was ~1.4 hours. Compared with the 4 d timescale of each experiment, this cycle time was short, such that changes in concentrations during passage through a treatment unit would be minor relative to the cumulative concentrations.

3.2. Effect of desorber temperature on N-nitrosamine formation from fresh MEA-based solvent

While *N*-nitrosamine formation in the absorber is driven by NO_x reactions with amines, nitrite reactions with amines under high temperature conditions drive *N*-nitrosamine formation in the desorber (Dai et al., 2012; Goldman et al., 2013; Dai and Mitch, 2014; Yu et al., 2017; Chen et al., 2018). To isolate the contribution of the absorber to *N*-nitrosamine formation within this continuously cycling pilot system, the desorber temperature was set to 45 °C, the same

290 temperature as the absorber, effectively negating its contribution (experiment 2 in Table 1 and
291 Figure 2b). Compared to the baseline condition (desorber at 110 °C; experiment 1), the nitrite
292 accumulation rate was ~50% higher, indicating that the heated desorber was a sink for nitrite.
293 However, the *N*-nitrosamine accumulation rates were similar, suggesting that NO_x reactions with
294 amines in the absorber unit drives *N*-nitrosamine formation from fresh MEA. One possible
295 explanation for the consumption of nitrite within the heated desorber unit without a
296 complementary increase in *N*-nitrosamine accumulation is that nitrosation of MEA occurs,
297 followed by rapid decay of the unstable primary *N*-nitrosamines (Mirvish, 1975). While this
298 nitrosation would serve to promote MEA degradation, and nitrosatable secondary amines occur
299 as degradation products of MEA (Strazisar et al., 2003; Gouedard et al., 2012; Vevelstad et al.,
300 2014; Einbu et al., 2015), higher concentrations of secondary amine degradation products may be
301 needed to observe significant formation of stable secondary *N*-nitrosamines within the desorber;
302 experiments testing this hypothesis with either simulated aged MEA solvent or the secondary
303 amine, PZ, are described below. A complementary experiment started with the desorber at 45 °C
304 for the first 48 hours and then the desorber was held at 110 °C for the remainder of the
305 experiment (Figure 3a). The *N*-nitrosamine accumulation rate remained constant, but the nitrite
306 accumulation rate decreased when the desorber temperature increased, consistent with

307 experiments 1 and 2 (Figures 2a and 2b). Although there were previous bench-scale experimental
308 results using separate absorber column and autoclaving treatments that indicated that *N*-
309 nitrosamine formation from fresh MEA was more significant in the absorber than in the desorber
310 (Dai and Mitch, 2013; Wang and Mitch, 2015), the current results verified this using experiments
311 with interconnected absorber and desorber units.

312 When the desorber temperature was set at 130 °C (experiment 3 in Table 1, Figure 2c), *N*-
313 nitrosamine accumulation rates from fresh MEA solvent decreased two-fold, but there was no
314 difference in nitrite accumulation rates. This decrease concurs with a previous experiment
315 conducted using another model of the same pilot rig, where *N*-nitrosamine accumulation from a
316 MEA-based solvent decreased as the desorber temperature increased from 120 to 140 °C (Einbu
317 et al., 2013). However, in that study, the two temperatures were investigated in sequence on the
318 same solvent as part of a 14-week campaign with substantial MEA degradation prior to the
319 temperature increase, which renders it difficult to isolate the effect of desorber temperature. As
320 indicated from experiments 1 and 2, *N*-nitrosamine formation from nitrite-MEA reactions in the
321 desorber was relatively unimportant for fresh MEA solvent. Autoclave-like experiments have
322 demonstrated that thermal decomposition of *N*-nitrosamines can be a possible sink for *N*-
323 nitrosamines at desorber-relevant temperatures (Fowler and Tobin, 1954; Tall and Zeman, 1985;

Fine et al., 2014b). The kinetics of *N*-nitrosamine thermal decomposition were proposed to be first-order, with rate constants depending on *N*-nitrosamine structure and temperature (Chandan et al., 2013; Fine et al., 2014a; Voice et al., 2015). The *N*-nitrosamines formed from MEA are a complex array of mostly unidentified molecules (Strazisar et al., 2003; Gouedard et al., 2012; Einbu et al., 2013; Vevelstad et al., 2014). However, Fine et al. (2014b) reported that *N*-nitroso-(2-hydroxyethyl)glycine and *N*-nitrosodiethanolamine, two representative *N*-nitrosamines derived from MEA, could undergo thermal decomposition at temperatures above 120 °C, concurring with our results and those of a previous study (Einbu et al., 2013).

3.3. Effects of NO_x composition and O_2/CO_2 ratio for the fresh MEA-based solvent

We had previously evaluated the effect of flue gas composition on *N*-nitrosamine formation from morpholine, a secondary amine similar in structure to piperazine (Dai and Mitch, 2014). While further validating the effects of desorber temperature, we sought to characterize the effects of flue gas composition on *N*-nitrosamine formation from fresh MEA, as a model primary amine. Similar to experiments 1 and 3, but at much higher NO_x concentrations (125 ppmv NO and 125 ppmv NO_2), *N*-nitrosamine accumulation rates dropped two-fold with little difference in nitrite accumulation rates when the desorber temperature increased from 110 °C to 130 °C (experiments 6 and 7 in Table 1).

Based upon four different NO_x concentrations in the synthetic flue gas at a desorber temperature of 110 °C (experiments 1, 4-6), the accumulation of *N*-nitrosamines and nitrite from fresh MEA solvent appeared to be simultaneously controlled by both NO and NO_2. By comparing experiments 1 and 4, and experiments 5 and 6, sets which had the same total NO_x concentration, the flue gas with the higher fraction of NO_2 consistently produced more *N*-nitrosamines as well as nitrite. Those observations are consistent with our bench-scale absorber-only experiments conducted using morpholine, a secondary amine that can directly form a stable *N*-nitrosamine, and by holding one NO_x species constant while varying the other (Dai and Mitch, 2014). In that previous study, the *N*-nitrosamine formation rates were linearly dependent on the individual NO and NO_2 concentrations, but much more sensitive to NO_2 than NO (Dai and Mitch, 2014). The first order dependence of *N*-nitrosamine formation with respect to both NO and NO_2 served as the basis to infer that N_2O_3, formed by the reaction between NO and NO_2, was the dominant nitrosating agent. Note that in experiment 4, which included 20 ppmv NO, but no NO_2, the nitrite accumulation rate (0.71 μM/h) was 77% of the value (0.92 μM/h on average) observed in the presence of both NO and NO_2 (experiment 1). These results suggest that NO can be a significant source of nitrite accumulation, presumably via NO oxidation to NO_2, NO_2 absorption into the solvent, and subsequent reactions involving hydrolysis of a N_2O_3 intermediate (equation

3). Previous molecular modeling and experimental validations also confirmed that NO_2 is not necessary for nitrosamine formation in CO_2 capture systems, with the potential for direct nitrosation of amines by NO (Shi et al., 2017; Supap et al., 2017).

Experiment 5 had NO and NO_2 concentrations that were both 12.5-fold higher than those in experiment 1. Appling the rate law obtained from morpholine (Dai and Mitch, 2014) to MEA in the present test rig experiments, we would expect the *N*-nitrosamine accumulation rate to be 156-fold higher in experiment 5 than experiment 1. However, the *N*-nitrosamine accumulation rate was only 8-fold higher, consistent with a previous study using the same type of rig, where increasing both NO and NO_2 by a factor 10 only promoted *N*-nitrosamine accumulation from MEA by just less than 10-fold instead of 100-fold (Haugen et al., 2012; Einbu et al., 2013). However, in the previous study the NO_x concentration was changed as part of a 14-week campaign on the same solvent, making it difficult to isolate the effects of NO_x from the accumulation of MEA degradation products. These results suggest a clear difference regarding the effect of NO_x on *N*-nitrosamine accumulation from primary and secondary amines. It is important to note that *N*-nitrosamine formation from primary amines requires initial formation of secondary amine precursors for *N*-nitrosamines by oxidative degradation of the primary amines (Fostas et al., 2011; Vevelstad et al., 2013). Thus, while N_2O_3 likely remains the primary

nitrosating agent in the absorber, oxidative degradation of the primary amine may be rate-limiting. Although a dependence on both NO and NO_2 remain, further studies that screen different combinations of NO and NO_2 concentrations over wider ranges would be needed to better resolve the numerical relationship between *N*-nitrosamine formation rates and NO_x composition for primary amines such as MEA.

We evaluated O_2/CO_2 ratios of 3 (12% O_2 and 4% CO_2) and 0.18 (2.4% O_2 and 13.5% CO_2), relevant to natural gas and coal combustion flue gases, respectively. The effect of desorber temperature on *N*-nitrosamine and nitrite accumulation rates for experiments 8, 10 and 11, conducted at the lower O_2/CO_2 ratio, were generally consistent with their counterparts at the higher O_2/CO_2 ratio (experiments 1-3). Increasing the desorber temperature from 45 °C to 110 °C decreased the nitrite accumulation rate, but did not affect the *N*-nitrosamine accumulation rate, validating the importance of the absorber unit for *N*-nitrosamine formation from fresh MEA. Increasing the desorber temperature to 130 °C did not affect the nitrite accumulation, but decreased the *N*-nitrosamine accumulation rate by more than two-fold, suggesting the importance of thermal decomposition of *N*-nitrosamines.

While the trends with respect to desorber temperature were the same for different O_2/CO_2 ratios, the lower ratio relevant to coal combustion consistently led to slower *N*-nitrosamine

accumulation than the natural gas counterpart (comparing experiments 1 and 8, 5 and 9, 2 and 10, and 3 and 11 in Table 1). The O_2/CO_2 ratio was less important for nitrite accumulation rates, although the accumulation rate decreased two-fold for the lower O_2/CO_2 ratio at the higher NO_x conditions (experiments 5 and 9). Although both experimental and computational evidence suggest that CO_2 could inhibit nitrosation in the absorber when carbamate formation protects the amine group (Versteeg et al., 1996; Kirsch et al., 2000), the increase in flue gas CO_2 concentration from 4.0% (natural gas) to 13.5% (coal) did not affect the steady-state CO_2 loadings for MEA in the rig experiments. Higher CO_2 concentrations could also reduce *N*-nitrosamine formation by increasing bicarbonate scavenging of N_2O_3 (Caulfield et al., 1996; Sun et al., 2011), but *N*-nitrosamine formation rates from morpholine within an absorber column were observed to be insensitive to this range of CO_2 concentrations (Dai and Mitch, 2014). These factors suggest that the lower *N*-nitrosamine accumulation rate was attributable to the lower O_2 concentration. Oxygen could promote nitrosation by transforming NO to NO_2, possibly forming more nitrosating agents (N_2O_3) (Goldstein and Czapski, 1996; Kirsch et al., 2000), and/or enhance MEA oxidative degradation, possibly forming more nitrosatable precursors (Vevelstad et al., 2013; Fine et al., 2014a). Indeed, previous research demonstrated that the *N*-nitrosamine formation rate depends on O_2 concentration for fresh MEA (Wang and Mitch, 2015) but not for

409 morpholine (Dai and Mitch, 2014). The present results from the rig experiments were consistent
410 with the interpretation that O_2 promotes *N*-nitrosamine formation from MEA by accelerating
411 amine degradation.

412 *3.4. Importance of absorber vs. desorber units for N-nitrosamine formation from fresh*
413 *piperazine*

414 Using a 1 M PZ solvent, the desorber temperature was set at either 45 °C or 110 °C
415 (experiments 12 and 13) to isolate the importance of the absorber. Compared with fresh MEA,
416 the *N*-nitrosamine accumulation rates for PZ were slightly higher when the desorber was set to
417 45 °C. Considering that the MEA concentration (5 M) was five-fold higher than the PZ
418 concentration (1 M), these results concur with previous results indicating the significantly higher
419 *N*-nitrosamine formation potential for secondary amines under absorber conditions (Dai and
420 Mitch, 2013; Chandan et al., 2013; Wang and Mitch, 2015). *N*-Nitrosamine accumulation rates
421 increased significantly at the higher desorber temperature (more than 5-fold higher than for 5 M
422 MEA), and there was a noticeable acceleration over time, possibly due to the net accumulation of
423 nitrite (Figure 2d). While there was little change in nitrite accumulation rates for different
424 desorber temperatures, this rate was higher than for 5 M MEA. The higher nitrite accumulation
425 rate may be associated with the lower PZ concentration, reducing the probability of PZ reaction

426 with NO_x in the absorber in favor of nitrite formation by hydrolysis of N_2O_3. These results were
427 further validated with an experiment in which the desorber was set to 45 °C for 48 hours and
428 then increased to 110 °C for the remainder of the experiment (Figure 3b). While the nitrite
429 accumulation rate did not change, the *N*-nitrosamine accumulation rate increased rapidly and
430 accelerated over time. These results suggest that the desorber served as the primary source of *N*-
431 nitrosamine formation for PZ.

432 Attempts to operate the desorber at 130 °C with 1 M PZ failed due to the inability of the
433 column seals to operate with this solvent under these conditions. However, previous research
434 using autoclave-like conditions indicated that *N*-nitrosopiperazine undergoes thermal degradation
435 at 120 °C (half-life ~1.5 days), and degrades faster at higher temperatures (half-life ~7 hours at
436 150 °C) (Fine et al., 2014b; Voice et al., 2015). Unlike MEA, *N*-nitrosamine formation in the
437 desorber is important for PZ, suggesting that higher desorber temperatures may increase *N*-
438 nitrosamine formation. Further research is needed at desorber temperatures of 120-150 °C to
439 characterize the balance between enhanced *N*-nitrosopiperazine formation from nitrite, and *N*-
440 nitrosopiperazine thermal degradation as a function of temperature.

441 *3.5. Simulated aged MEA solvent*

442 The contrast between the importance of the absorber unit for *N*-nitrosamine formation from
443 fresh MEA (Figure 3a), a primary amine, and the desorber unit for *N*-nitrosamine formation from
444 fresh piperazine (Figure 3b), a secondary amine, suggested that the relative importance of the
445 units may change as MEA solvent accumulates secondary amine degradation products over time.
446 A synthetic aged MEA solvent was concocted using 5 M MEA spiked with 3 mM nitrite and 75
447 mM sarcosine (1.5% of the total amines) as a model secondary amine. These nitrite (Strazisar et
448 al., 2003) and secondary amine (Einbu et al., 2013) concentrations approximate levels observed
449 in previous long-term pilot tests involving MEA solvent. Oxidative degradation of MEA
450 produces a complex mixture of amine products (Saeed et al., 2018). Previous research
451 demonstrated that nitrosamine formation from sarcosine was within a factor of five of that
452 observed for other secondary amines (e.g., diethanolamine and piperazine) under both absorber
453 and desorber relevant conditions (Dai and Mitch, 2013). To mimic NO_x conditions relevant to
454 practice, the influent flue gas contained 18 ppmv NO and 320 ppmv NO_2 (experiments 14 and 15
455 in Table 1). After merging with the recirculated gas, the elevated NO_2 concentration would yield
456 ~2 ppmv NO_2 if all of the NO_2 absorbed into the solvent with each passage through the absorber
457 unit; as discussed previously, NO is poorly soluble. The desorber temperature was increased
458 from 45 °C to 110 °C halfway through the experiment (Figure 4).

With the high initial nitrite concentration, the rate of increase in nitrite concentration was too small over the course of the experiment to be significant by linear regression, and did not appear to change drastically with the change in desorber temperature. When the desorber was set at 45 °C to isolate *N*-nitrosamine formation in the absorber unit, the *N*-nitrosamine accumulation rate (0.67 μM/h) was comparable to the rate observed with fresh MEA in experiment 6; although the desorber was set to 110 °C in experiment 6, *N*-nitrosamine formation within the desorber was not important for fresh MEA (Figure 3a). Experiments 6 and 15 are difficult to compare since the concentrations of NO, NO_2 and sarcosine differed, but clearly NO_2 was an important contributor to *N*-nitrosamine formation in the absorber. After the desorber was heated to 110 °C (experiment 14), the rate of *N*-nitrosamine accumulation increased by an order of magnitude for the aged MEA solvent, but did not change for the fresh MEA solvent (compare Figures 3a and 4), suggesting that the desorber unit dominates *N*-nitrosamine formation in the aged MEA solvent, with the amended 75 mM sarcosine, not the 5 M MEA, serving as the predominant precursor. The secondary amine degradation products forming from MEA can vary with time and operating conditions (Gouedard et al., 2012), but if sarcosine serves as a representative secondary amine product, these results suggest that *N*-nitrosamine formation should shift from the absorber to the desorber unit as MEA degradation produces mM levels of secondary amines.

3.6. Test rig vs. autoclave treatments

One critical question is the extent to which the use of separate absorber and autoclave-like desorber mimics characterizes *N*-nitrosamine accumulation within more realistic interconnected absorber and desorber systems. Samples collected from the test rig partway through an experiment (Figures 3 and 4) were autoclaved for 3 h. We compared the amounts of *N*-nitrosamines produced during the autoclave treatment (yellow diamonds in Figures 3 and 4) with those formed during the continued operation of the test rig. For this comparison, the total *N*-nitrosamines formed after the 3 h autoclave were plotted at 6 h after the samples were collected from the rig, since the solvent spends roughly 50% of its time in the desorber unit within the rig, and so 3 h of desorber treatment is equivalent to 6 h of continuous cycling. Moreover, the total *N*-nitrosamine concentration measured after the autoclave treatment was increased by the *N*-nitrosamine formation expected to result from the 3 h of exposure in the absorber unit, based on the linear formation rate observed when the desorber was at 45 °C (this increase was less than 10% of the total). These total *N*-nitrosamine levels were compared against the levels interpolated from the measurements collected from the rig (Figures 3 and 4).

For fresh MEA, there was no significant difference between *N*-nitrosamine formation in the test rig or after autoclave treatment (Figure 3a), as expected since *N*-nitrosamine formation

associated with the desorber was of negligible importance for fresh MEA. For the secondary amine, PZ, the autoclave treatment correctly indicated that the *N*-nitrosamine concentration would increase, but underestimated *N*-nitrosamine concentrations relative to those observed in the rig (Figure 3b). *N*-Nitrosamine concentrations increased from 4 μM to 5 μM (25% increase) during autoclaving, but would have increased to ~9 μM (125% increase) based on the trend observed within the test rig. Similar underestimation of *N*-nitrosamine formation by autoclave treatments was seen in the experiment with simulated aged MEA (Figure 4). Although the cause is unclear, changes in nitrite between the two systems likely can not explain this difference, since the additional nitrite accumulation associated with the ~3 h of additional NO_x absorption in the test rig would be minor compared to the levels already present in the solvent when the samples were taken. We speculate that one other important difference between the two systems is the significantly higher interfacial surface areas between the gas and liquid phases in the test rig (counter-current system with Raschig rings) relative to the autoclave (stagnant liquid in a vial with headspace). Although a mechanism is unclear, one possibility is that gas phase species promote *N*-nitrosamine formation in the desorber. Evaluating this is technically challenging due to the difficulty of promoting higher interfaces within the autoclave (e.g., by purging a recirculated gas).

Conclusions

This study is one of the first to systematically investigate *N*-nitrosamine formation using interconnected absorber and desorber units encompassing a wide range of operation conditions. Our results indicate that *N*-nitrosamine formation from fresh MEA is dominated by reactions with NO_x in the absorber unit. Although nitrite is consumed within the desorber unit, *N*-nitrosamine formation within this unit was relatively unimportant. For the secondary amine, PZ, the *N*-nitrosamine accumulation rate was higher, despite the five-fold lower amine concentration in the solvent. Moreover, *N*-nitrosamine accumulation was dominated by reactions with nitrite in the desorber unit, accelerating over time together with the accumulation of nitrite in the solvent. These results suggest that the nitrite consumption in the desorber unit observed with fresh MEA solvent was associated with MEA degradation, perhaps via formation of unstable primary *N*-nitrosamine intermediates. When the MEA solvent contained mM level accumulated nitrite and 1.5% sarcosine as a model for secondary amine degradation products that might accumulate as degradation products in aged MEA solvent, *N*-nitrosamine accumulation rates increased and the dominant locus for *N*-nitrosamine formation shifted to the desorber unit.

For MEA, operation of the desorber unit at 130 °C reduced *N*-nitrosamine accumulation rates by 50%, concurring with other research indicating that operating the desorber unit at

temperatures above 120 °C may thermally degrade *N*-nitrosamines (Einbu et al., 2013; Fine et al., 2014b; Voice et al., 2015). Although we were unable to evaluate PZ at that temperature, the ability of this strategy to mitigate *N*-nitrosamine accumulation should be further evaluated, since higher desorber temperatures may also promote *N*-nitrosopiperazine production from nitrite (Chandan et al., 2013; Fine et al., 2014a). The critical temperature required to facilitate net decomposition also has to be evaluated in the context of overall energy efficiency and amine stability.

Lastly, the prevalent practice of using separate absorber columns and autoclave-like mimics for desorber units can indicate whether desorber units will promote *N*-nitrosamine formation, although with some underestimation. Certainly, separate absorber unit and autoclave-like mimics are simpler to operate and do not require an expensive pilot test rig. Additionally, they can cleanly isolate effects associated with absorber and desorber units. However, it is also important to capture the magnitude of processes, particularly when evaluating the net impacts of opposing processes (e.g., *N*-nitrosamine formation vs. thermal degradation in the desorber).

Acknowledgements

This work was funded by the Stanford Woods Institute for the Environment and National Natural Science Foundation of China (21806021). The test rig used in the present study was a gift from the CO_2 Capture Mongstad (CCM) Project in Norway. We appreciate the technical support of Royal Kopperud and Bill Sabala at Stanford and Powerspan Corporation at New Hampshire. The comments and suggestions from the anonymous reviewers improved an earlier version of the manuscript.

Supporting Information

This supporting information is available on line.

References

Ali Mazari, S., Alaba, P., Saeed, I. M., 2019. Formation and elimination of nitrosamines and nitramines in freshwaters involved in post-combustion carbon capture process. J. Environ. Chemo. Eng.: DOI: 10.1016/j.jece.2019.103111.

Barzagli, F., Mani, F., Peruzzini, M., 2016. A comparative study of the CO_2 absorption in some solvent-free alkanolamines and in aqueous monoethanolamine (MEA). *Environ. Sci. Technol.* 50, 7239-7246.

Bishnoi, S., Rochelle, G. T., 2000. Absorption of carbon dioxide into aqueous piperazine: reaction kinetics, mass transfer and solubility. *Chem. Eng. Sci.* 55, 5531-5543.

Casado, J., Mosquera, M., Paz, L. C., Prieto, M. F. R., Tato, J. V., 1984. Nitrite ion as a nitrosating reagent. Nitrosation of morpholine and diethylamine in the presence of formaldehyde. *J. Chem. Soc., Perkin Trans.* 2 12, 1963-1966.

Caulfield, J. L., Singh, S. P., Wishnok, J. S., Deen, W. M., Tannenbaum, S. R., 1996. Bicarbonate inhibits N-nitrosation in oxygenated nitric oxide solutions. *J. Biol. Chem.* 271, 25859-25863.

Challis, B. C., Kyrtopoulos, S. A., 1976. Nitrosation under alkaline conditions. *J. Chem. Soc., Chem. Commun.* 21, 877-878.

Chandan, P. A., Remias, J. E., Neathery, J. K., Liu, K., 2013. Morpholine nitrosation to better understand potential solvent based CO_2 capture process reactions. *Environ. Sci. Technol.* 47, 5481-5487.

Chen, X., Huang, G., An, C., Yao, Y., Zhao, S., 2018. Emerging N-nitrosamines and N-nitramines from amine-based post-combustion CO_2 capture–a review. *Chem. Eng. J.* 335, 921-935.

Chi, S.; Rochelle, G. T., 2002. Oxidative degradation of monoethanolamine. *Ind. Eng. Chem. Res.* 41, 4178-4186.

Clark, V. R., Herzog, H. J., 2014. Assessment of the US EPA's determination of the role for CO_2 capture and storage in new fossil fuel-fired power plants. *Environ. Sci. Technol.* 48, 7723-7729.

Clesceri, L.; Greenberg, A.; Eaton, A., 1998. *Standard methods for the examination of water and wastewater*. American Public Health Association, American Water Works Association, and Water Environment Association: Washington DC, USA.

Cousins, A., Cottrell, A., Lawson, A., Huang, S., Feron, P. H., 2012. Model verification and evaluation of the rich-split process modification at an Australian-based post combustion CO_2 capture pilot plant. *Greenhouse Gas. Sci. Technol.* 2, 329-345.

Cousins, A., Nielsen, P. T., Huang, S., Rowland, R., Edwards, B., Cottrell, A., Chen, E., Rochelle, G. T., Feron, P. H. M., 2015, Pilot-scale evaluation of concentrated piperazine for CO2

602 capture at an Australian coal-fired power station: Nitrosamine measurements. *Int. J. Greenh. Gas.*
603 *Con.* 37, 256-263.
604
605 Dai, N., Shah, A. D., Hu, L., Plewa, M. J., McKague, B., Mitch, W. A., 2012. Measurement of
606 nitrosamine and nitramine formation from NO_x reactions with amines during amine-based
607 carbon dioxide capture for postcombustion carbon sequestration. *Environ. Sci. Technol.* 46,
608 9793-9801.
609
610 Dai, N.; Mitch, W. A., 2013. Influence of amine structural characteristics on N-nitrosamine
611 formation potential relevant to postcombustion CO_2 capture systems. *Environ. Sci. Technol.* 47,
612 13175-13183.
613
614 Dai, N., Mitch, W. A., 2014. Effects of flue gas compositions on nitrosamine and nitramine
615 formation in postcombustion CO_2 capture systems. *Environ. Sci. Technol.* 48, 7519-7526.
616
617 de Koeijer, G., Enge, Y., Sanden, K., Graff, O. F., Falk-Pedersen, O., Amundsen, T., Overå, S.,
618 2011. CO_2 Technology Centre Mongstad–Design, functionality and emissions of the amine plant.
619 *Energy Procedia* 4, 1207-1213.
620
621 Dong, C., Huang, G., Cheng, G., Yao, Y., Chen, X., Chen, J., 2019. Wastewater treatment in
622 amine-based carbon capture. *Chemosphere* 222, 742-756.
623
624 Dutcher, B., Fan, M., Russell, A. G., 2015. Amine-based CO_2 capture technology development
625 from the beginning of 2013—A Review. *ACS Appl. Mater. Interfaces* 7, 2137-2148.
626
627 Einbu, A., DaSilva, E., Haugen, G., Grimstvedt, A., Lauritsen, K. G., Zahlsen, K., Vassbotn, T.,
628 2013. A new test rig for studies of degradation of CO2 absorption solvents at process conditions;
629 comparison of test rig results and pilot plant data for degradation of MEA. *Energy Procedia* 37,
630 717-726.
631
632 Fine, N. A., Rochelle, G. T., 2014. Absorption of nitrogen oxides in aqueous amines. *Energy*
633 *Procedia* 63, 830-847.
634
635 Fine, N. A., Goldman, M. J., Rochelle, G. T., 2014a. Nitrosamine formation in amine scrubbing
636 at desorber temperatures. *Environ. Sci. Technol.* 48, 8777-8783.

Fine, N. A., Nielsen, P. T., Rochelle, G. T., 2014b. Decomposition of nitrosamines in CO2 capture by aqueous piperazine or monoethanolamine. *Environ. Sci. Technol.* 48, 5996-6002.

Finlayson-Pitts, B., Wingen, L., Sumner, A., Syomin, D., Ramazan, K., 2003. The heterogeneous hydrolysis of NO_2 in laboratory systems and in outdoor and indoor atmospheres: An integrated mechanism. *Phys. Chem. Chem. Phys.* 5, 223-242.

Fostås, B., Gangstad, A., Nenseter, B., Pedersen, S., Sjøvoll, M., Sørensen, A. L., 2011. Effects of NOx in the flue gas degradation of MEA. *Energy Procedia* 4, 1566-1573.

Fowler, J. P., Tobin, M. C., 1954. The thermal decomposition of cyclotrimethylenetrinitrosamine. *J. Phys. Chem.* 58, 382-383.

Freeman, S. A., Dugas, R., Van Wagener, D. H., Nguyen, T., Rochelle, G. T., 2010. Carbon dioxide capture with concentrated, aqueous piperazine. *Int. J. Greenh. Gas. Con.* 4, 119-124.

Ge, X., Shaw, S. L., Zhang, Q., 2014. Toward understanding amines and their degradation products from postcombustion CO2 capture processes with aerosol mass spectrometry. *Environ. Sci. Technol.* 48, 5066-5075.

Glover, C.M., Verdugo, E.M., Trenholm, R.A., Dickenson, E.R., 2019. N-nitrosomorpholine in potable reuse. *Water Res.* 148, 306-313.

Goldman, M. J., Fine, N. A., Rochelle, G. T., 2013. Kinetics of N-nitrosopiperazine formation from nitrite and piperazine in CO_2 capture. *Environ. Sci. Technol.* 47, 3528-3534.

Goldstein, S., Czapski, G., 1996. Mechanism of the nitrosation of thiols and amines by oxygenated NO solutions: the nature of the nitrosating intermediates. *J. Am. Chem. Soc.* 118, 3419-3425.

Gouedard, C., Picq, D., Launay, F., Carrette, P.-L., 2012. Amine degradation in CO_2 capture. I. A review. *Int. J. Greenh. Gas. Con.* 10, 244-270.

Hamborg, E. S., Smith, V., Cents, T., Brigman, N., Falk-Pedersen, O., De Cazenove, T., Chhaganlal, M., Feste, J. K., Ullestad, Ø., Ulvatn, H., 2014. Results from MEA testing at the CO_2 Technology Centre Mongstad. Part II: Verification of baseline results. *Energy Procedia* 63, 5994-6011.

Haugen, G., Einbu, A., Chikukwa, A., da Silva, E. F., Grimstvedt, A., 2012. *Process Protocol*; SINTEF F22608; Trondheim, Norway, 2012-04-27.

Idem, R., Supap, T., Shi, H., Gelowitz, D., Ball, M., Campbell, C.; Tontiwachwuthikul, P. 2015. Practical experience in post-combustion CO_2 capture using reactive solvents in large pilot and demonstration plants. *Int. J. Greenh. Gas Con.*, 40, 6-25.

Keefer, L. K., Roller, P. P., 1973. N-nitrosation by nitrite ion in neutral and basic medium. *Science* 181, 1245-1247.

Kirsch, M., Korth, H.-G., Sustmann, R., De Groot, H., 2000. Carbon dioxide but not bicarbonate inhibits N-nitrosation of secondary amines. Evidence for amine carbamates as protecting entities. *Chem. Res. Toxicol.* 13, 451-461.

Maree, Y., Nepstad, S., de Koeijer, G., 2013. Establishment of knowledge base for emission regulation for the CO_2 technology centre Mongstad. *Energy Procedia* 37, 6265-6272.

Mirvish, S. S., 1975. Formation of N-nitroso compounds: Chemistry, kinetics, and in vivo occurrence. *Toxicol. Appl. Pharmacol.* 31, 325-351.

Nielsen, P. T., Li, L., Rochelle, G. T., 2013. Piperazine degradation in pilot plants. *Energy Procedia* 37, 1912-1923.

Reynolds, A. J., Verheyen, T. V., Adeloju, S. B., Meuleman, E., Feron, P., 2012. Towards commercial scale postcombustion capture of CO_2 with monoethanolamine solvent: key considerations for solvent management and environmental impacts. *Environ. Sci. Technol.* 46, 3643-3654.

Rochelle, G. T., 2009. Amine scrubbing for CO_2 capture. Science 325, 1652-1654.

Strazisar, B. R., Anderson, R. R., White, C. M., 2003. Degradation pathways for monoethanolamine in a CO_2 capture facility. *Energy Fuels* 17, 1034-1039.

Saeed, I. M., Alaba, P., Ali Mazari, S., Basirun, W. J., Lee, V. S., Sabzoi, N., 2018. Opportunities and challenges in the development of monoethanolamine and its blends for post-combustion CO_2 capture. *Int. J. Greenh. Gas Con.* 79, 212-233.

Shi, H., Supap, T., Idem, R., Gelowitz, D., Campbell, C., Ball, M., 2017. Nitrosamine formation in amine-based CO_2 capture in the absence of NO_2: Molecular modeling and experimental validation. *Environ. Sci. Technol.* 51, 7723-7731.

Sun, Z., Liu, Y. D., Zhong, R. G., 2011. Carbon dioxide in the nitrosation of amine: catalyst or inhibitor? *J. Phys. Chem. A* 115, 7753-7764.

Supap, T., Shi, H., Idem, R., Gelowitz, D., Campbell, C. Ball, M., 2017. Nitrosamine formation mechanism in amine-based CO_2 capture: Experimental validation. *Energy Procedia*, 114, 952-958.

Tall, A., Zeman, S., 1985. Thermal decomposition of some nitrosamines. *Thermochim. Acta* 93, 25-28.

Versteeg, G., Van Dijck, L., Van Swaaij, W., 1996. On the kinetics between CO2 and alkanolamines both in aqueous and non-aqueous solutions. An overview. *Chem. Eng. Commun.* 144, 113-158.

Vevelstad, S. J., Grimstvedt, A., Elnan, J., da Silva, E. F., Svendsen, H. F., 2013. Oxidative degradation of 2-ethanolamine: The effect of oxygen concentration and temperature on product formation. *Int. J. Greenh. Gas. Con.* 18, 88-100.

Vevelstad, S.J., Grimstvedt, A., Haugen, G., Kupfer, R., Brown, N., Einbu, A., Vernstad, K., Zahlsen, K., 2017. Comparison of different solvents from the solvent degradation rig with real samples. *Energy Procedia*, 114, 2061-2077.

Vevelstad, S. J., Grimstvedt, A., Knuutila, H., da Silva, E. F., Svendsen, H. F., 2014. Influence of experimental setup on amine degradation. *Int. J. Greenh. Gas. Con.* 28, 156-167.

Voice, A. K., Hill, A., Fine, N. A., Rochelle, G. T., 2015. Nitrosamine formation and mitigation in blended amines for CO2 capture. *Int. J. Greenh. Gas. Con.* 39, 329-334.

Wang, Z., Mitch, W. A., 2015. Influence of dissolved metals on N-Nitrosamine formation under amine-based CO_2 capture conditions. *Environ. Sci. Technol.* 49, 11974-11981.

Weiland, R. H., Trass, O., 1969. Titrimetric determination of acid gases in alkali hydroxides and amines. *Anal. Chem.* 41, 1709-1710.

Yu, K., Mitch, W.A., Dai, N., 2017. Nitrosamines and nitramines in amine-based carbon dioxide capture systems: fundamentals, engineering implications and knowledge gaps. *Environ. Sci. Technol.* 51, 11522-11536.

Yu, Q., Wang, P., Ma, F., Xie, H.B., He, N., Chen, J. 2017. Computational investigation of the nitrosation mechanism of piperazine in CO_2 capture. *Chemosphere* 186, 341-349.

Zhao, B., Nakada, N., Okumura, K., Zhou, J. Tanaka, H. 2019. N-nitrosomorpholine behavior in sewage treatment plants and urban rivers. *Water Res.* 163, 114868.

Zhou, Y., Rao, Y., Wang, T., Jens, K.J. 2018. Influence of formaldehyde on N-nitrosopiperazine formation from nitrite and piperazine in CO_2 capture. *Int. J. Greenh. Gas Con.*, 69, 36-40.

764 **Figure Captions**

765

766 **Figure 1.** Simplified schematic of the test rig that allowed for continuous operation of carbon
767 capture tests with solvent cycling between the absorber and desorber. A and B represent sample
768 locations for lean and rich solvents, respectively.

769

770 **Figure 2.** Accumulation of *N*-nitrosamines and nitrite in the test rig using fresh 5 M MEA with
771 the desorber temperature at 110 °C (a), 45 °C (b) and 130 °C (c). Panel d is for the experiment
772 using 1 M PZ with the desorber temperature at 110 °C and note the different timescale of the x-
773 axis. The flue gas composition was at baseline conditions. Red and blue symbols indicate *N*-
774 nitrosamine and nitrite concentrations, respectively. Circle and triangle symbols indicate
775 concentrations measured at sampling ports A (desorber) and B (absorber), respectively. Panel a
776 includes a replicate data set (Exp. 1b) presented with symbols without borders. Lines serve as
777 visual guides for the trends.

778 **Figure 3.** Dynamics of *N*-nitrosamine and nitrite concentrations in the test rig with initial
779 desorber temperature at 45 °C and later at 110 °C for experiments with fresh 5 M MEA (a) and 1
780 M PZ (b). The vertical dashed lines indicate the change of desorber temperature. Red and blue
781 symbols indicate *N*-nitrosamine and nitrite concentrations, respectively. Circle and triangle
782 symbols indicate concentrations at sampling ports A (desorber) and B (absorber), respectively.
783 The yellow diamond symbols indicate the final concentrations of *N*-nitrosamines after 3-hour
784 autoclave treatment of the samples taken from the test rig. As the 3-hour autoclave treatment was
785 equivalent to 6 hours in the test rig (half of the residence time was in the desorber), on the x-axis
786 the yellow diamond symbols were placed at 6 hours after the samples were collected from the rig
787 prior to autoclaving. Lines serve as visual guides for the trends. The yellow arrows provide
788 visual guidance for the time span and the *N*-nitrosamine production with respect to the autoclave
789 treatment.

790

Figure 4. Dynamics of *N*-nitrosamine and nitrite concentrations with initial desorber temperature at 45 °C and later at 110 °C for experiments with simulated aged MEA solvent containing 5 M MEA, 75 mM sarcosine and 3 mM nitrite. The vertical dashed line indicates the change of desorber temperature. Red and blue symbols indicate *N*-nitrosamine and nitrite concentrations, respectively. Circle and triangle symbols indicate concentrations at sampling ports A (desorber) and B (absorber), respectively. The yellow symbols indicate the final concentrations of *N*-nitrosamines after 3-hour autoclave treatment of the samples taken from the test rig. As the 3-hour autoclave treatment was equivalent to 6 hours in the test rig (half of the residence time was in the desorber), on the x-axis the yellow diamond symbols were placed at 6 hours after the samples were collected from the rig prior to autoclaving. Lines serve as visual guides for the trends. The yellow arrows provide visual guidance for the time span and the *N*-nitrosamine production with respect to the autoclave treatment.

Table 1. Summary of the experiments conducted using the advanced test rig[a]

ID	Desorber T (°C)	NO (ppmv)	NO_2 (ppmv)	O_2/CO_2	N-nitrosamine (μM/h)	Nitrite (μM/h)	Comment
Baseline							
1a	110	18	2	3	0.055	0.90	Baseline for
1b	110	18	2	3	0.059	0.94	Natural flue gas
Effect of Desorber T							
2	45	18	2	3	0.063	1.5	No desorber
3	130	18	2	3	0.033	0.91	High desorber T
Effect of NO_x							
4	110	20	0	3	0.033	0.71	Removal of NO_2
5	110	225	25	3	0.47	6.9	High NO_x
6	110	125	125	3	0.87	19	High NO_x and NO_2
7	130	125	125	3	0.35	16	High T, NO_x and NO_2
Effect of O_2/CO_2							
8	110	18	2	0.18	0.021	0.77	Compare with baseline
9	110	225	25	0.18	0.29	3.8	Typical coal flue gas
10	45	18	2	0.18	0.022	1.4	No desorber
11	130	18	2	0.18	0.013	1.0	High desorber T
Piperazine							
12	110	18	2	3	> 0.40[b]	1.9	Regular operation
13	45	18	2	3	0.077	2.0	No desorber
Simulated aged MEA[c]							
14	110	18	320[c]	3	4.2	n.s. [d]	Regular operation
15	45	18	320[c]	3	0.67	n.s. [d]	No desorber

a. N_2 was fixed at 84%. The sum of CO_2 and O_2 was fixed at 16%. The rationales to select those flue gas conditions were described in Table S1. Liquid flow rates are shown in Figure 1. The total flue gas flow rate is 22 L/h and the actual gas flow rate in the absorber column in combination with the fan recycle is 3500 L/h. Additional data are shown in Figure S2.
b. The *N*-nitrosamine formation rate from PZ in Exp. 12 was accelerating. The value was calculated using the last two data points and it is anticipated that the rate would further increase as nitrite continued to accumulate.
c. The initial solvent contained 3 mM nitrite and 75 mM sarcosine. The high NO_2 influent concentration was targeted to approximate a 2 ppmv concentration reaching the absorber column, assuming all of the NO_2 is lost to the solvent during each pass of gas through the column. See Section 2.4 for further discussion. These experiments were conducted with the same solvent sequentially, starting with experiment 15 and then 14.
d. n.s. = not significant. The initial nitrite concentration was too high to permit observation of a significant increase in nitrite concentration over the course of the experiment.

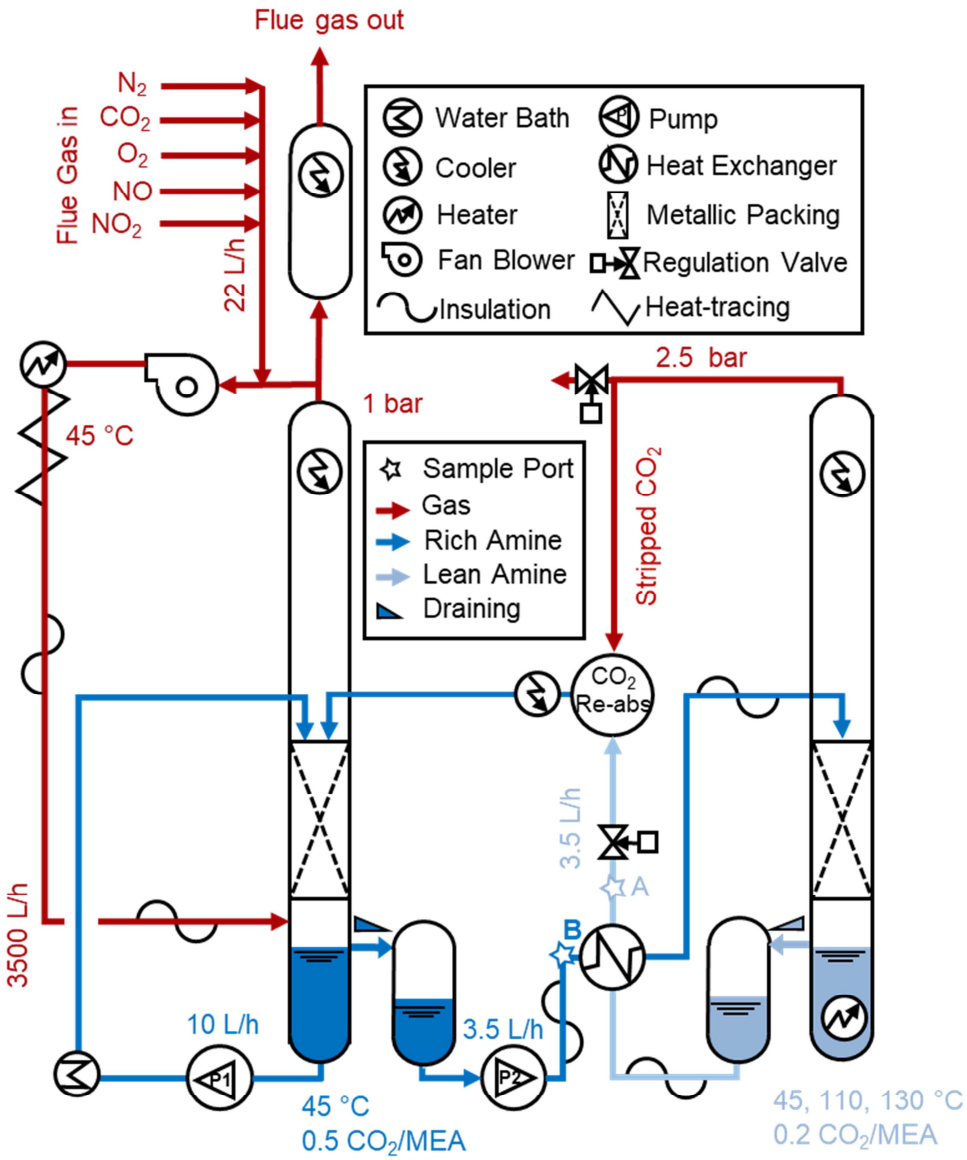

Figure 1. Simplified schematic of the test rig that allowed for continuous operation of carbon capture tests with solvent cycling between the absorber and desorber. A and B represent sample locations for lean and rich solvents, respectively.

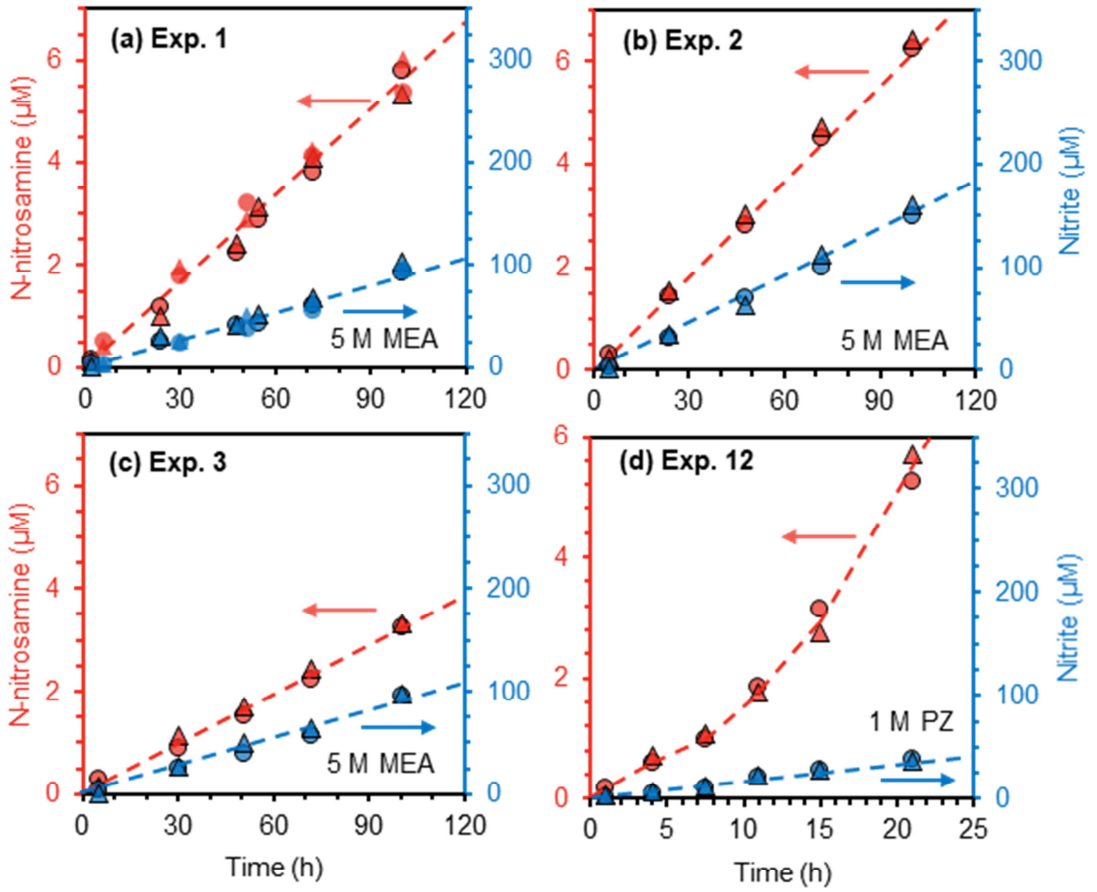

Figure 2. Accumulation of *N*-nitrosamines and nitrite in the test rig using fresh 5 M MEA with the desorber temperature at 110 °C (a), 45 °C (b) and 130 °C (c). Panel d is for the experiment using 1 M PZ with the desorber temperature at 110 °C and note the different timescale of the x-axis. The flue gas composition was at baseline conditions. Red and blue symbols indicate *N*-nitrosamine and nitrite concentrations, respectively. Circle and triangle symbols indicate concentrations measured at sampling ports A (desorber) and B (absorber), respectively. Panel a includes a replicate data set (Exp. 1b) presented with symbols without borders. Lines serve as visual guides for the trends.

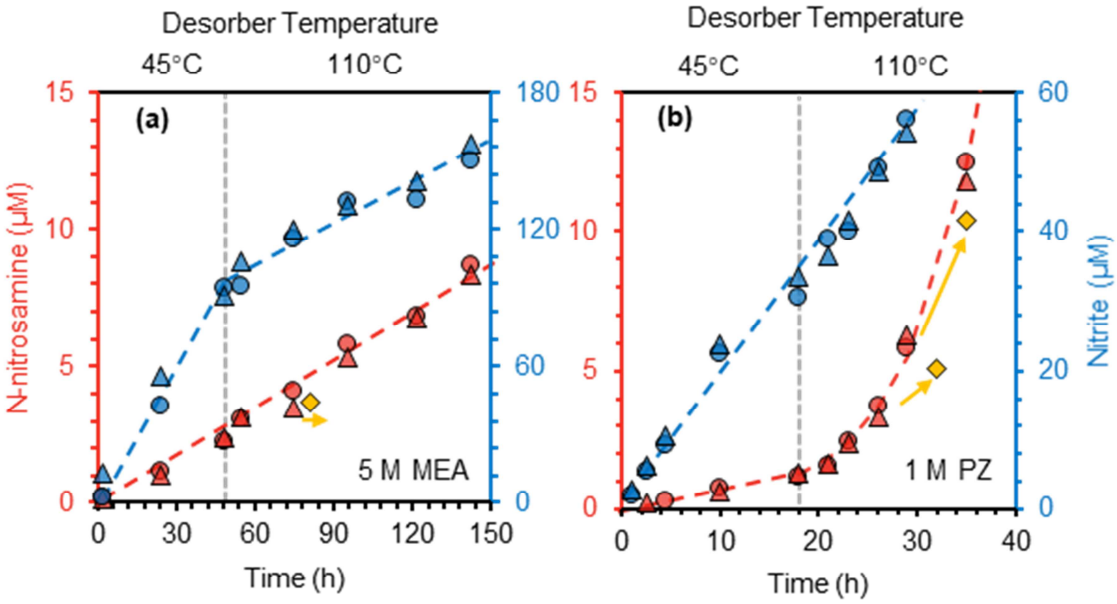

Figure 3. Dynamics of *N*-nitrosamine and nitrite concentrations in the test rig with initial desorber temperature at 45 °C and later at 110 °C for experiments with fresh 5 M MEA (a) and 1 M PZ (b). The vertical dashed lines indicate the change of desorber temperature. Red and blue symbols indicate *N*-nitrosamine and nitrite concentrations, respectively. Circle and triangle symbols indicate concentrations at sampling ports A (desorber) and B (absorber), respectively. The yellow diamond symbols indicate the final concentrations of *N*-nitrosamines after 3-hour autoclave treatment of the samples taken from the test rig. As the 3-hour autoclave treatment was equivalent to 6 hours in the test rig (half of the residence time was in the desorber), on the x-axis the yellow diamond symbols were placed at 6 hours after the samples were collected from the rig prior to autoclaving. Lines serve as visual guides for the trends. The yellow arrows provide visual guidance for the time span and the *N*-nitrosamine production with respect to the autoclave treatment.

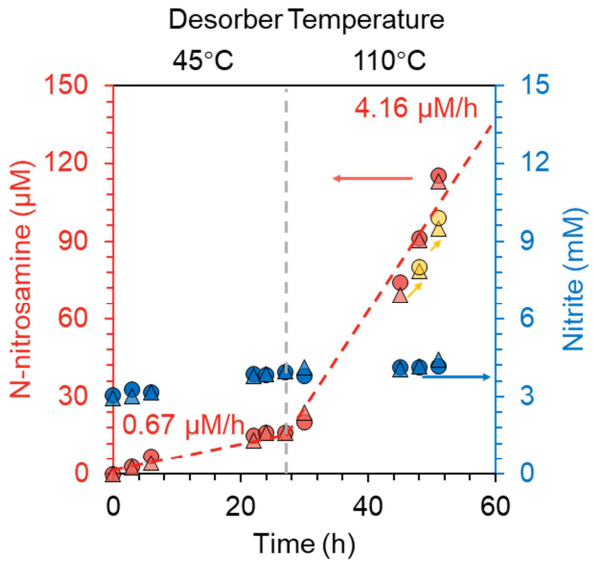

Figure 4. Dynamics of *N*-nitrosamine and nitrite concentrations with initial desorber temperature at 45 °C and later at 110 °C for experiments with simulated aged MEA solvent containing 5 M MEA, 75 mM sarcosine and 3 mM nitrite. The vertical dashed line indicates the change of desorber temperature. Red and blue symbols indicate *N*-nitrosamine and nitrite concentrations, respectively. Circle and triangle symbols indicate concentrations at sampling ports A (desorber) and B (absorber), respectively. The yellow symbols indicate the final concentrations of *N*-nitrosamines after 3-hour autoclave treatment of the samples taken from the test rig. As the 3-hour autoclave treatment was equivalent to 6 hours in the test rig (half of the residence time was in the desorber), on the x-axis the yellow diamond symbols were placed at 6 hours after the samples were collected from the rig prior to autoclaving. Lines serve as visual guides for the trends. The yellow arrows provide visual guidance for the time span and the *N*-nitrosamine production with respect to the autoclave treatment.

Highlights

A test rig with absorber-desorber cycling evaluated nitrosamine formation

Nitrosamine formation from fresh MEA was driven by NO_x/O_2 in the absorber

Nitrosamine formation from PZ and simulated aged MEA was driven by the desorber

Using autoclaves to mimic desorber units underestimated nitrosamine formation

Declaration of interests

☒ The authors declare that they have no known competing financial interests or personal relationships that could have appeared to influence the work reported in this paper.

☐The authors declare the following financial interests/personal relationships which may be considered as potential competing interests: